CHEMISTRY OF MATERIALS

Article

On the Formation Mechanism of Freestanding CH3NH3PbI3 Functional Crystals: in situ Transformation vs Dissolution-Crystallization

Shuang Yang, Yi Chu Zheng, Yu Hou, Xiao Chen, Ying Chen, Yun Wang, Huijun Zhao, and Hua Gui Yang

Chem. Mater., **Just Accepted Manuscript** • DOI: 10.1021/cm5028817 • Publication Date (Web): 14 Nov 2014

On the Formation Mechanism of Freestanding $CH_3NH_3PbI_3$ Functional Crystals: *in situ* Transformation vs Dissolution-Crystallization

Shuang Yang,[†] Yi Chu Zheng,[†] Yu Hou,[†] Xiao Chen,[†] Ying Chen,[†] Yun Wang,[‡] Huijun Zhao,[‡] and Hua Gui Yang*[,†,‡]

[†] Key Laboratory for Ultrafine Materials of Ministry of Education School of Materials Science and Engineering East China University of Science and Technology, 130 Meilong Road, Shanghai, 200237 (China)

[‡] Centre for Clean Environment and Energy, Gold Coast Campus Griffith University, Queensland, 4222, (Australia)

KEYWORDS: perovskite, organic-inorganic hybrid composites, *in situ* transformation, dissolution-crystallization, crystal growth

ABSTRACT: To date, the formation mechanism of organolead halide $CH_3NH_3PbI_3$ perovskites based on the efficient sequential reaction route, has remained virtually unexplored. Such a synthetic method usually yields high-performance solar cells with an efficiency over 15%, and the identification of the crystal growth mechanism is crucial for understanding the chemical reaction process and further improving the light converting efficiency. Herein, we develop a versatile and facile approach based on sequential reaction to produce freestanding $CH_3NH_3PbI_3$ crystals as a model for crystal growth mechanism studies. It was found that the *in situ* transformation and dissolution-crystallization mechanisms play competing roles in determining the characteristics of products that are largely depend on the chemical reaction kinetics. Such a method can also be readily used for synthesis of freestanding $CH_3NH_3PbI_3$ crystals with controllable morphological characteristics, such as cuboids, rods, wires, and plates. The synthetic strategy as well as the crystal growth mechanisms exemplified here can also serve in the design and development of more sophisticated organolead halide perovskites as well as further optimization across a range of possible domains of applications.

1. INTRODUCTION

Organic-inorganic perovskites have drawn intensive research interests for their successfully coupling of the advantages of organic and inorganic components.[1-5] Among these materials, the $CH_3NH_3PbX_3$ (X=Cl, Br or I) perovskites have made a breakthrough as the sensitizer of solar cells recently. [6-11] In pursuit of high-performance devices, several synthetic methods have been explored to prepare organolead halide perovskite films. Generally, there are two ways for preparing organolead halide perovskite films. One is the one-step spin-casting route which usually yields inhomogeneous morphological structures because of the uncontrollable precipitation.[12-15] Another is the sequential deposition route by reacting pre-deposited PbX_2 film with CH_3NH_3X isopropanol solution or gaseous molecules.[6, 16-18] This simple method has led to the impressive efficiency over 15% with optimized pore filling and full coverage of the films.[6]

Despite the success of sequential reaction in photovoltaic devices, the corresponding knowledge of the inherent process of crystal growth is highly desired and crucial for the synthesis of organic-inorganic perovskites and further designing improved functional materials. Conventionally, this sequential reaction is ideally deemed to be an *in situ* intercalation mechanism via the insertion of organic ammonium cations.[19] However, the previous understandings ignored the complexity of this reaction, such as the solvation or dissolution of lead halides, coordinative change of metal ions, insertion of the organic cations and structural reconstruction. In fact, all these issues are still absent in the literature, and thus we sought to systematically probe the crystal growth mechanism which can provide further advancement of these functional materials. In addition, freestanding perovskite crystals are also essential due to the ease of being measured as basic prototype for the fundamental research compared with thin films as well as their potential applications.

Herein, we firstly developed a versatile and facile method based on sequential reaction for preparing solution-processed freestanding $CH_3NH_3PbI_3$ crystals which acted as the experimental prototype for studying the crystal formation mechanism. Our further experimental results illustrated that crystal growth is in line with a competing relation between *in situ* transformation and dissolution-crystallization mechanisms, which is largely dependent on the reaction

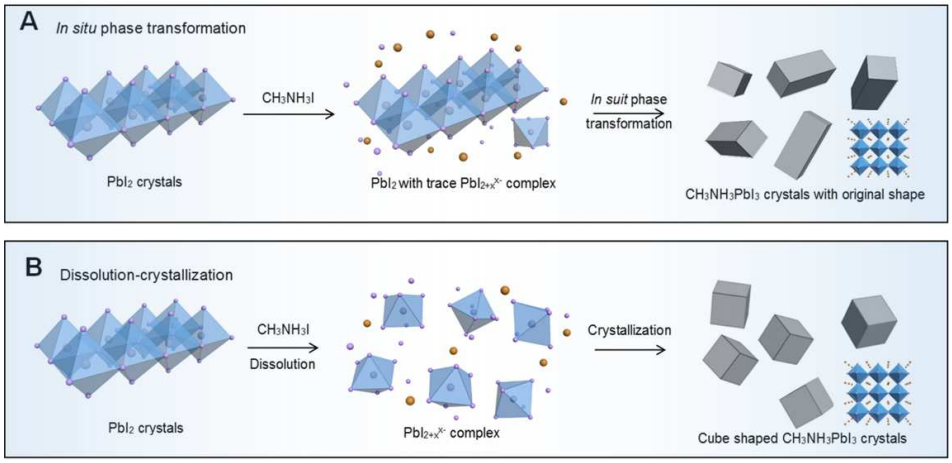

Figure 1. Schematic illustration of the plausible formation mechanisms of (A) *in situ* transformation and (B) dissolution-crystallization of $CH_3NH_3PbI_3$ crystals via sequential reaction route. The insets in the right images are the atomic structure of $CH_3NH_3PbI_3$ crystals.

kinetics by governing the chemical coordination between Pb and I atoms. To the best of our knowledge, such crystal growth mechanism has not been reported for this important sequential reaction process of organic-inorganic perovskite crystals. Moreover, the freestanding perovskite crystals can not only be kept parallel geometries to PbI_2, but reconstructed into cube-shaped perovskite crystals as well at certain CH_3NH_3I concentration. Our synthesis strategy would enable the availability of freestanding perovskite crystals with controllably geometries as well as understanding the intrinsic crystal growth of organic-inorganic perovskites.

2. EXPERIMENTAL SECTION

2.1. Synthesis of PbI_2 crystals. Lead iodine crystals were synthesized by a modified method according to the literature.[25] Typically, 0.971 g lead nitrate ($Pb(NO_3)_2$, 99%, Aldrich) and certain amount of the capping agents were dissolved in 25 ml deionized water. Here, the capping agents for the synthesis of sample PbI_2-S1 and PbI_2-S2 are 0.06 g of polyvinyl pyrrolidone (PVP, M=40000, Aldrich), 0.10 g of cetyltrimethylamonium bromide (CTAB, 99%, Aldrich), respectively, and the sample PbI_2-S3 is synthesized without capping agents. Then 5 mL of 0.6 M potassium iodide (KI, 99%, Aldrich) aqueous solution which acted as iodine precursor was slowly dropped into the $Pb(NO_3)_2$ solution under vigorous stirring at 700 rpm, and a yellow coloured precursor was obtained. The mixture of 30 ml was transferred into a Teflon-lined autoclave with a filling ratio of 60%. The vessel was then sealed and treated at 120 °C for 12 h in an oven. After cooled to room temperature, the clear solution at the upper section was carefully removed by plastic dropper and a precipitate (PbI_2 product) formed at the bottom of the Teflon reactor. The solid products obtained were collected by centrifugation at 7000 rpm for 6 min, raised with H_2O twice (15 ml each time) and dried at 60 °C in a vacuum oven overnight.

2.2. Synthesis of freestanding $CH_3NH_3PbI_3$ crystals. CH_3NH_3I was synthesized according to the literature by a solution reaction of 24 mL methylamine solution (33 wt% in ethanol, Aldrich), 10 mL hydroiodic acid (HI, 57 wt%, Aldrich) and 100 mL ethanol (99.7%, Shanghai Lingfeng Chemical reagent) in 250 mL round bottomed flask under nitrogen atmosphere at 0 °C for 2 h with stirring at 400 rpm.[11] The precipitate was recovered by evaporation at 50 °C for 2 h, washed with diethyl ether three times and finally dried at 60 °C in vacuum oven overnight. The synthesis of $CH_3NH_3PbI_3$ was conducted via a sequential reaction route at room temperature. In a typical synthesis, 2 mg of PbI_2 was firstly added in 2 ml isopropanol (IPA, 99.7%, Aldrich). These PbI_2 crystals can not be dissolved and to ensure well dispersion, the obtained suspension was further treated in ultrasonic bath for 15 min. Then 8 mL of 20.06 mM CH_3NH_3I isopropanol solution was dropwise added into the PbI_2 suspension under magnetic stirring at 400 rpm. The colour of the precipitates changed from yellow to dark brown and finally to black. After stirring for 2 h, the products were separated by centrifugation at 7000 rpm for 6 min, washed three times with hexane or chlorobenzene (10 ml each time) and finally dried at 60 °C for 2h in a vacuum oven.

2.3. Material characterization. Crystallographic information of $CH_3NH_3PbI_3$ crystals was investigated by powder X-ray diffraction (PXRD, Bruker D8 Advanced Diffractometer, Cu Kα radiation, 40 kV). The morphology and structure of the samples were characterized by field emission scanning electron microscopy (FESEM, HITACHI S4800) and transmission electron microscopy (TEM, JEOL JEM-1400, 100 kV). PbI_2 and perovskite samples were dispersed in deionized water or hexane, respcetively, and then dropped on a conductive SEM sample holder, or a carbon-coated copper grid with irregular holes for electron microscopy (SEM/TEM) analysis. The Pb content dissolved in solution was determined by inductively coupled plasma spectroscopy (ICP). The optical absorption spectra were measured by using a Cary 500 Spectrophotometer. The photofluorescence spectra were obtained from a Fluorolog-3-P molecular fluorescence spectrometer with excitation wavelength of 460 nm.

3. RESULTS AND DISCUSSION

Typically, crystal growth in solution can be classified into

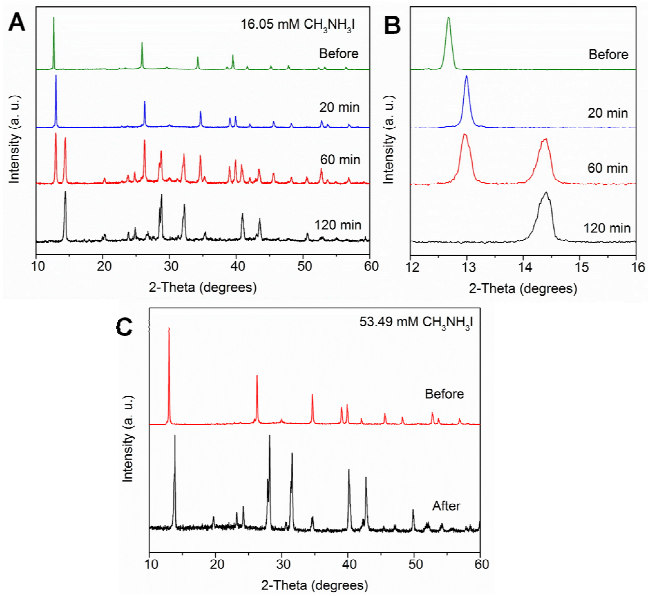

Figure 2. PXRD patterns of the $CH_3NH_3PbI_3$ crystals synthesized with different concentration of CH_3NH_3I: (A, B) 16.05, and (C) 53.49 mM. (B) shows detailed patterns around 12° and 16° 2θ values.

three basic types: precipitation from supersaturated solution, *in situ* transformation, and dissolution-crystallization.[20] Regarding the reaction conditions for the sequential process, it should be processed by *in situ* transformation or dissolution-crystallization mechanisms as shown in Figure 1. Here, PbI_2 is a layered semiconductor contains a hexagonally closed-packed Pb plane sandwiched between two layers of iodide ions. For the *in situ* transformation mechanism, only trace amount of PbI_2 will be dissolved in solvent which suggests the inorganic lead framework can be remained. The dissolved iodine ions would drive edge-sharing PbI_6 octahedrons to corner-sharing structure along the equatorial direction, together with the inserting of the organic ammonium ions. Generally, PbI_2 is almost completely insoluble in isopropanol that the lead framework has been presumed to be remained, however, in this case, it can be truly coordinated with iodine ions to form lead complex.[21-23] Therefore, we hypothesize that the crystal growth of perovskites would undergo a dissolution-crystallization process in iodine rich environment. In the presence of ammonium cations, coordinated lead complex as building blocks can further recrystallize into a thermodynamically favored morphology.[24]

Our synthetic strategy of $CH_3NH_3PbI_3$ crystals typically involves initial preparation of PbI_2 crystals with expected geometries based on a hydrothermal method by reacting $Pb(NO_3)_2$ with KI in the presence of capping agents.[25] Then the PbI_2 crystals were transferred into an isopropanol solution with excess CH_3NH_3I, these crystals were therefore turned from yellow to dark brown and finally to black. There is also some difference between PbI_2 samples in the transformation rate which is probably ascribed to the shape, size, and surface characteristics of PbI_2 and the CH_3NH_3I concentration.

During the formation of perovskite crystals, iodine ions play crucial roles to determine the crystal growth mechanism; it is thus necessary to investigate the crystallographic variations of the products with different I^- concentration. Figure 2 presents the PXRD patterns of the products by reacting as-prepared sample PbI_2-S1 with 16.05 and 53.49 mM CH_3NH_3I in isopropanol. Diffraction peaks at 12.67°, 25.51°, 38.66° and 52.39° match well with the (001), (002), (003) and (004) lattice planes of hexagonal 2H PbI_2 polytype (space group: *P3m1*(164), JCPDS file No. 07-0235), respectively. After reacting for 20 min in 16.05 mM CH_3NH_3I, the diffraction peaks shift to about 0.35° larger 2-theta values which may be as a consequence of the coordinate variation of lead and intercalation of interstitial molecules, ions or atoms forming a transient state. Further reaction to 60 min, the obtained crystals exhibit two separated phase of PbI_2 and $CH_3NH_3PbI_3$ accompanied by the CH_3NH_3I intercalation. We then observed the almost completely formation of perovskite phase at 120 min, and the refined tetragonal lattice parameters, a=8.762(2) Å, c=12.449(5) Å, are slightly smaller than the previous reported values.[16, 26] The presence of vacancies on one or two of the three primitive sites of perovskites may locally cause the alternating of crystal lattice in an attempt to reestablish stoichiometry across all the site,[27] since the long reaction time for $CH_3NH_3PbI_3$ indicates the deficiency of $CH_3NH_3^+$ and I^- kinetically. Evidently, this crystallization process should be an *in situ* transformation rather than dissolution-crystallization due to the presence of the transient state between the networks of edge sharing hexagonal and

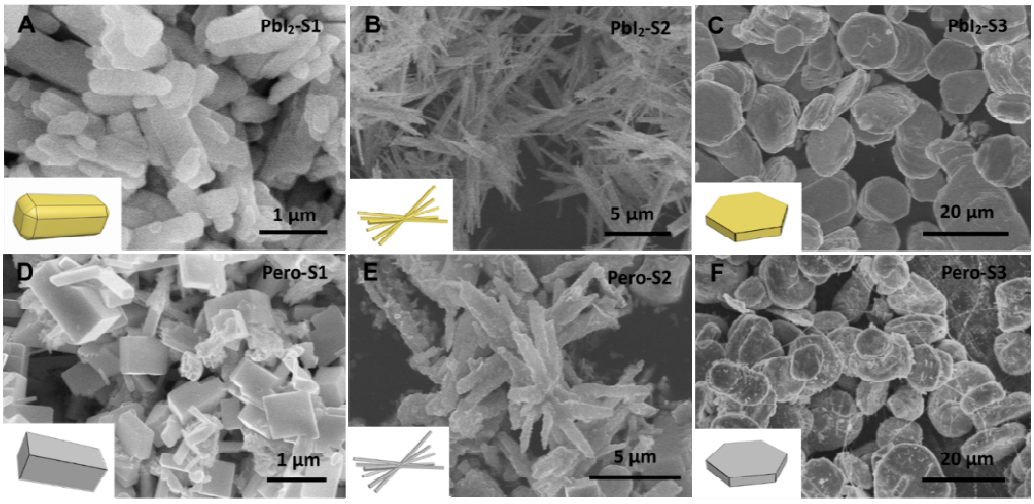

Figure 3. SEM images of the as prepared (A-C) PbI_2 and (D-F) $CH_3NH_3PbI_3$ crystals. The insets are the corresponding shape models. All samples were synthesized with the reaction time of 2 h.

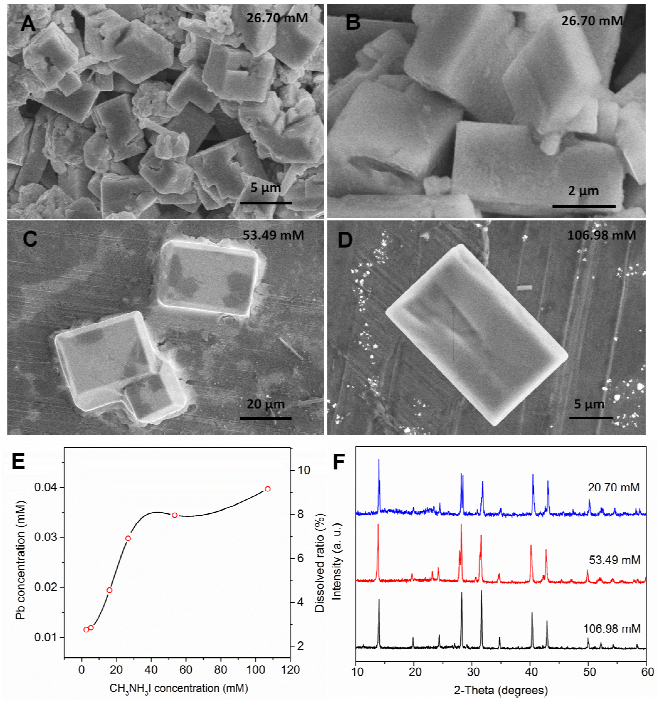

Figure 4. (A-D) SEM images of the $CH_3NH_3PbI_3$ crystals obtained with different CH_3NH_3I concentration. (B) is at high magnification of the sample in (A). (E) Relationship between the dissolved Pb concentration (left axis) and ratio (right axis) versus CH_3NH_3I concentration in the system after reaction. (F) PXRD patterns of the $CH_3NH_3PbI_3$ crystals synthesized with different CH_3NH_3I concentration.

corner sharing tetragonal PbI_6 octahedrons both at 20 and 60 min. Additionally, the scanning electron microscopy (SEM) images of the products harvested at different reaction times clearly illustrated the *in situ* transformation was firstly occurred at the crystal surface by gradual ions intercalation with the original lead framework (Figure S1). However, when 53.49 mM CH_3NH_3I was used, the precipitate turned black within seconds and in principle, such rapid crystal growth would result in the collapse of the lead backbones. Only tetragonal phase $CH_3NH_3PbI_3$ occurred even in short reaction time, and considering the extra iodine ions can coordinate with Pb atoms,[21] this process should be classified as dissolution-crystallization.

One inherent difference between above mechanisms lies in keeping or collapse of the lead framework before and after reaction, which can be associated with the morphological change. To enable systematical observation of these changes, PbI_2-S1, PbI_2-S2, and PbI_2-S3 were synthesized with PVP, CTAB or without capping agents by a hydrothermal method which present rod, wire and plate shapes, respectively (Figure 3). After the reaction in 16.05 mM CH_3NH_3I, the lead framework of Pero-S1 is still kept as the rod shaped PbI_2-S1 with the similar size and the crystals exhibits well-defined cuboid surface with edges and corners. The sample Pero-S2 and Pero-S3 are kept well of their overall wire and plate shapes with PbI_2 crystals and are also confirmed by transmission electron microscopy (TEM) images (Figure S2). Interestingly, although the reaction conditions were kept constant in these experiments, a small amount of PbI_2 is still existed in Pero-S3, which may be due to the difference in crystal geometries (Figure S3). Certainly, all three samples prepared at low CH_3NH_3I concentration are in good consistent with the *in situ* transformation mechanism, and we have therefore demonstrated a new synthetic strategy to prepare $CH_3NH_3PbI_3$ crystals with targeted geometric characteristics, in which the overall crystal shapes are largely dependent on the morphology of PbI_2 crystals.

To elucidate the dissolution-crystallization mechanism, we then sought to increase the CH_3NH_3I concentration, which is expected to destabilize PbI_2 lattice and favor the recrystallization into thermodynamically geometries. Inductively coupled plasma (ICP) spectroscopy was employed to determine the amount of Pb dissolved of PbI_2-S1 sample at different CH_3NH_3I concentration as shown in Figure 4e. We found that PbI_2 is tend to be dissolved in iodine rich condition and such phenomenon can be fulfilled by following chemical equation,[21]

$$PbI_2 + xI^- \rightleftharpoons PbI_{2+x}^{x-} \quad (x = 1, 2) \qquad (1)$$

The morphological and crystallographic information in such process were further investigated by SEM and PXRD, and the results are shown in Figure 4. With CH_3NH_3I in the range between 2.67 and 5.34 mM, the amount of dissolved lead was detected to be lower than 0.0121 mM or 2.85% in the isopropanol solution that resulted in incomplete formation of perovskites. Curiously, when using 26.07 mM CH_3NH_3I, rod shaped crystals can not be observed, and alternatively, totally new cube shaped $CH_3NH_3PbI_3$ crystals with mean size of

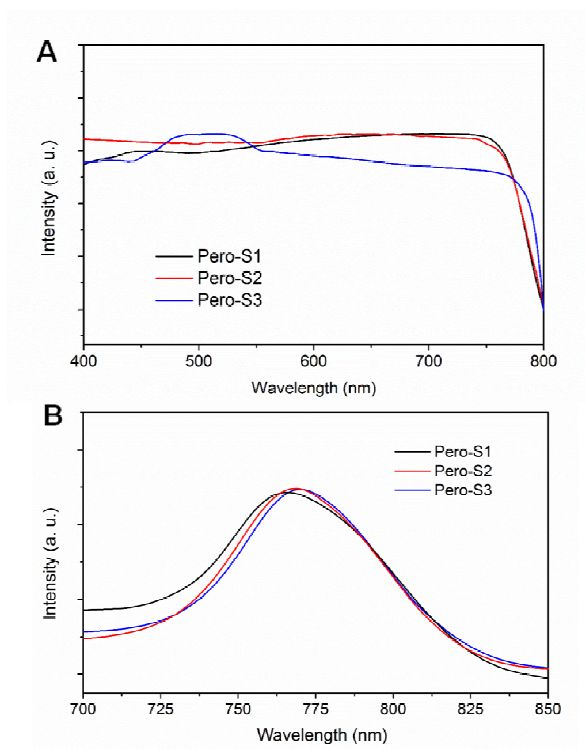

Figure 5. (A) UV–*vis* absorption and (B) photoluminescence spectrum of the as prepared $CH_3NH_3PbI_3$ perovskites.

4.13 μm were generated, suggesting the intensive dissolution of PbI_2 framework and the following recrystallization into $CH_3NH_3PbI_3$ crystals (Figure S4). Furthermore, by using 53.49 mM CH_3NH_3I, the mean size of obtained $CH_3NH_3PbI_3$ crystals reaches a maximum of 30.2 μm with tetragonal structure as we expected in the dissolution-crystallization growth. We finally raised the CH_3NH_3I concentration to 106.98 mM, which inversely reduces the cube shaped crystals to a mean size of 15.4 μm.

As suggested above, our experimental results agree well with the previous result that the PbI_2 can be isolated into PbI_3^- or PbI_4^{2-} complex in iodine rich environment, as the first dissolution step according to equation (1).[21] The formation of Pb complex would shift the equilibrium forward to form perovskites via the recrystallization step of equation (2).

$$CH_3NH_3^- + PbI_{2+x}^{x-} \rightleftharpoons CH_3NH_3PbI_3 + (x-1)I^-(x=1,2) \quad (2)$$

On the basis of these findings, it can be reasonably concluded that the kinetics of such crystal growth process is greatly relied on the CH_3NH_3I concentration. At low CH_3NH_3I concentration (<16.5 mM), only a small amount of PbI_2 can be bonded with iodine ions to form PbI_3^- and/or PbI_4^{2-} complex, and the lead framework can be preserved. Subsequently, the recrystallization can not be fully conducted and reversely, the $CH_3NH_3I^+$ and I^- are more prone to be directly intercalated into the lead frameworks which give rise to $CH_3NH_3PbI_3$ crystals with original shapes by the *in situ* transformation. However, the dissolved Pb concentration shows a slow change in the presence of sufficient CH_3NH_3I (>26.7 mM), indicating PbI_2 may be well coordinated and existed as PbI_4^{2-} form in this condition.[21] This also allows the synthesis of new cube shaped $CH_3NH_3PbI_3$ crystals whose size was firstly increased to a maximum of 30.2 μm and then reduced to 15.4 μm. Hence, the iodine ions act as both lead ligands and reaction products at high CH_3NH_3I concentration, which expedite the dissolution of lead iodine, reversely retard the bonding between each complex, and thus can finally regulate the crystal characteristics. Since dissolution can be occurred partly even in poor solvents, the main distinction between *in situ* transformation and dissolution-crystallization mechanism is the relative kinetic reaction rate of the dissolution-crystallization process.[20] Based on these systematically studies by measuring the solubility of PbI_2, the keep or collapse of lead backbone and the intermediate state during the reaction, we can reasonably concluded that *in situ* transformation and dissolution-crystallization play the dominate role at low and high CH_3NH_3I concentration, respectively. In addition, both mechanisms work together at the medial CH_3NH_3I concentration.

We then measured the UV-*vis* absorption and photoluminescence (PL) of the obtained $CH_3NH_3PbI_3$ perovskite crystals at room temperature as depicted in Figure 5. All $CH_3NH_3PbI_3$ crystals we synthesized have broad optical absorption up to 800 nm and most photons in the visible range can not propagate through such materials, and thus are localized and absorbed. However, we note that there are some differences the absorbance onset of the sample Pero-S3 as compared to Pero-S1 and S2, which may be as a result of the different crystal geometries.[28] Moreover, Pero-S3 has an absorption peak centered at 500 nm. This may be derived from the PbI_2 as a result of the incomplete reaction which is in consistence with recent reports.[29] The normalized near-infrared photoluminescence of the perovskite crystals is shown in Figure 4B. A 5 nm red shift in the emission peak from Pero-S1 (λ_{max} =766 nm) to Pero-S3 (λ_{max}=771 nm) can be observed in registry with the absorption spectrum. These optical differences probably arise from the size, shape, and polycrystalline of $CH_3NH_3PbI_3$ crystals as well as the existence of $PbI_2/CH_3NH_3PbI_3$ heterostructures. This difference also hold promise for the further optimization of this class of materials by crystal shape engineering or incorporation of heterostructures.

CONCLUSION

In summary, we have developed for the first time a versatile and simple synthetic strategy to prepare solution-processed freestanding $CH_3NH_3PbI_3$ perovskite crystals for revealing the intrinsic crystal growth mechanism. Different from the previous views, the experimental results presented here on cleaved samples illustrate vividly that the *in situ* transformation and dissolution-crystallization mechanisms play competing roles in perovskite crystal growth, which largely depends on iodine concentration that determine chemical reaction kinetics. Crucially, by controlling the PbI_2 morphology and CH_3NH_3I concentration, we have succeed in tailoring the crystal geometries including rods, wires, plates, and cubes with tunable size. For the similarity of this type of organic-inorganic perovskite based material, other organic-inorganic hybrid perovskites can be, in principle, obtained by this method accordingly. Furthermore, the $CH_3NH_3PbI_3$ crystals we synthesized exhibit significant difference in optical properties. These results indicate this method may help to understand the crystal growth mechanism of organolead halide perovskites which have potential applications such as catalysis, solar cells, field-effect transistors, light-emitting devices as well as other opto-electronic devices.

ASSOCIATED CONTENT

Supporting Information. Figures show SEM, TEM and PXRD of the resultant samples. This material is available free of charge via the Internet at http://pubs.acs.org.

AUTHOR INFORMATION

Corresponding Author

* E-mail: hgyang@ecust.edu.cn

ACKNOWLEDGMENT

This work was financially supported by National Natural Science Foundation of China (21373083, 21203061), SRF for ROCS, SEM, SRFDP, Programme for Professor of Special

Appointment (Eastern Scholar) at Shanghai Institutions of Higher Learning, Fundamental Research Funds for the Central Universities (WD1313009, WD1214036), and China Postdoctoral Science Foundation (2012M511056, 2013T60425).

REFERENCES

(1) Kagan, C.; Mitzi, D.; Dimitrakopoulos, C. *Science* **1999,** 286, 945-947.
(2) Mitzi, D. B. *J. Chem. Soc., Dalton Trans.* **2001**, 1-12.
(3) Mitzi, D. B. *J. Mater. Chem.* **2004,** 14, 2355-2365.
(4) Mitzi, D. B. *Prog. Inorg. Chem.* **2007**, 48, 1-121.
(5) Schmidt, L. C.; Pertegás, A.; González-Carrero, S.; Malinkiewicz, O.; Agouram, S.; Minguez Espallargas, G.; Bolink, H. J.; Galian, R. E.; Pérez-Prieto, J. *J. Am. Chem. Soc.* **2014,** 136, 850–853.
(6) Burschka, J.; Pellet, N.; Moon, S.-J.; Humphry-Baker, R.; Gao, P.; Nazeeruddin, M. K.; Grätzel, M. *Nature* **2013,** 499, 316-319.
(7) Liu, M.; Johnston, M. B.; Snaith, H. J. *Nature* **2013,** 501, 395–398.
(8) Kojima, A.; Teshima, K.; Shirai, Y.; Miyasaka, T. *J. Am. Chem. Soc.* **2009,** 131, 6050-6051.
(9) Jeon, N. J.; Lee, H. G.; Kim, Y. C.; Seo, J.; Noh, J. H.; Lee, J.; Seok, S. I. *J. Am. Chem. Soc.* **2014,** 136, 7837-7840.
(10) Xing, G.; Mathews, N.; Sun, S.; Lim, S. S.; Lam, Y. M.; Grätzel, M.; Mhaisalkar, S.; Sum, T. C. *Science* **2013,** 342, 344-347.
(11) Stranks, S. D.; Eperon, G. E.; Grancini, G.; Menelaou, C.; Alcocer, M. J.; Leijtens, T.; Herz, L. M.; Petrozza, A.; Snaith, H. J. *Science* **2013,** 342, 341-344.
(12) Eperon, G. E.; Burlakov, V. M.; Docampo, P.; Goriely, A.; Snaith, H. J. *Adv. Funct. Mater.* **2013,** 24, 151–157.
(13) Docampo, P.; Ball, J. M.; Darwich, M.; Eperon, G. E.; Snaith, H. J. *Nat. Commun.* **2013,** 4.
(14) Heo, J. H.; Im, S. H.; Noh, J. H.; Mandal, T. N.; Lim, C.-S.; Chang, J. A.; Lee, Y. H.; Kim, H.-j.; Sarkar, A.; NazeeruddinMd, K.; Gratzel, M.; Seok, S. I. *Nat. Photon.* **2013,** 7, 486–491.
(15) Conings, B.; Baeten, L.; De Dobbelaere, C.; D'Haen, J.; Manca, J.; Boyen, H.-G. *Adv. Mater.* **2013,** 26, 2041-2046.
(16) Liang, K.; Mitzi, D. B.; Prikas, M. T. *Chem. Mater.* **1998,** 10, 403-411.
(17) Chen, Q.; Zhou, H.; Hong, Z.; Luo, S.; Duan, H.-S.; Wang, H.-H.; Liu, Y.; Li, G.; Yang, Y. *J. Am. Chem. Soc.* **2013,** 136, 622-625.
(18) Cohen, B. E.; Gamliel, S.; Etgar, L. *APL Mat.* **2014**, 2, 081502.
(19) Mitzi, D. B. *Chem. Mater.* **2001,** 13, 3283-3298.
(20) Markov, I. V. *Crystal growth for beginners*. World Scientific, 1995.
(21) Horváth, O.; Mikó, I. *J. Photoch. Photobio. A* **1998,** 114, 95-101.
(22) Shaopu, L.; Yi, L.; Zhonfan, L. *Mikrochim. Acta* **1983,** 81, 355-366.
(23) Clever, H. L.; Johnston, F. J. *J. Phys. Chem. Ref. Data* **1980,** 9, 751-784.
(24) Lovette, M. A.; Browning, A. R.; Griffin, D. W.; Sizemore, J. P.; Snyder, R. C.; Doherty, M. F. *Ind. Eng. Chem. Res.* **2008,** 47, 9812-9833.
(25) Zhu, G.; Liu, P.; Hojamberdiev, M.; Zhou, J.-p.; Huang, X.; Feng, B.; Yang, R. *Appl. Phys. A Mater. Sci. Process.* **2010,** 98, 299-304.
(26) Colella, S.; Mosconi, E.; Fedeli, P.; Listorti, A.; Gazza, F.; Orlandi, F.; Ferro, P.; Besagni, T.; Rizzo, A.; Calestani, G.; Gigli, G.; De Angelis, F.; Mosca, R. *Chem. Mater.* **2013,** 25, 4613-4618.
(27) Neagu, D.; Tsekouras, G.; Miller, D. N.; Ménard, H.; Irvine, J. T. S. *Nat. Chem.* **2013,** 5, 916-923.
(28) Pan, J.; Liu, G.; Lu, G. Q.; Cheng, H.-M., *Angew. Chem. Int. Ed.* **2011,** 123, (9), 2181-2185.
(29) Chen, Q.; Zhou, H.; Song, T.-B.; Luo, S.; Hong, Z.; Duan, H.-S.; Dou, L.; Liu, Y.; Yang, Y. *Nano Letters* **2014,** 14, 4158-4163.

Shuang Yang, Yi Chu Zheng, Yu Hou, Xiao Chen, Ying Chen, Yun Wang, Huijun Zhao and Hua Gui Yang*

On the Formation Mechanism of Freestanding $CH_3NH_3PbI_3$ Functional Crystals: *in situ* Transformation vs Dissolution-Crystallization